Cell, Vol. 106, 633–645, September 7, 2001, Copyright ©2001 by Cell Press

Argosomes: A Potential Vehicle for the Spread of Morphogens through Epithelia

Valentina Greco, Michael Hannus, and Suzanne Eaton[1]
Max Planck Institute for Molecular Cell Biology and Genetics
Pfotenhauerstrasse-108
01307 Dresden
Germany

Summary

The formation of morphogen gradients is essential for tissue patterning. Morphogens are released from producing cells and spread through adjacent tissue; paradoxically, however, many morphogens, including Wingless, associate tightly with the cell membrane. Here, we describe a novel cell biological mechanism that disperses membrane fragments over large distances through the *Drosophila* imaginal disc epithelium. We call these membrane exovesicles argosomes. Argosomes are derived from basolateral membranes and are produced by many different regions of the disc. They travel through adjacent tissue where they are found predominantly in endosomes. Wingless protein colocalizes with argosomes derived from Wingless-producing cells. The properties of argosomes are consistent with their being a vehicle for the spread of Wingless protein.

Introduction

Pattern formation in developing tissues occurs in response to the graded distribution of morphogens such as Wingless, Hedgehog, and Decapentaplegic. Different levels of morphogen are thought to generate different patterns of transcriptional activity in responding cells, thus specifying differentiation programs that vary with distance from the morphogen-producing cells (Lawrence and Struhl, 1996; Neumann and Cohen, 1997; Christian, 2000). The final shape of the morphogen gradient is critical for elaboration of developmental pattern. Although simple diffusion was first proposed as a model to explain morphogen gradients, recently it has become clear that their shape is very carefully controlled both by morphogen-producing cells, and by the tissue through which morphogens travel. The long-range movement of Decapentaplegic requires the endocytic pathway in receiving cells (Entchev et al., 2000). The spread of the Hedgehog and Wingless proteins is modulated both by heparan sulfate proteoglycans (HSPGs), and by the level of their receptors. (Chen and Struhl, 1996; Bellaiche et al., 1998; Cadigan et al., 1998; Lin and Perrimon, 1999; Tsuda et al., 1999; Lin and Perrimon, 2000; Baeg et al., 2001)

Paradoxically, in spite of their ability to travel long distances, many morphogens are found tightly associated with membranes. Members of the Wnt family, including Wingless, bind tightly to HSPGs (Bradley and Brown, 1990; Papkoff and Schryver, 1990; Reichsman et al., 1996), and Hedgehog binds to membranes via covalently attached cholesterol and palmitate (Porter et al., 1996; Pepinsky et al., 1998). Nevertheless, all hypotheses proposed thus far to explain the spread of these molecules make the assumption that they are released from the membrane of producing cells. Since the generation of budded membrane vesicles forms the basis for several signaling events in the lymphocyte lineage (Denzer et al., 2000a), we wondered whether similar membrane vesiculation might provide a vehicle for the spread of morphogens. To test this idea, we examined membrane dynamics in the *Drosophila* wing imaginal disc epithelium by expressing a glycophosphatidylinositol (gpi) linked GFP in subsets of disc cells.

Results

Studies of Membrane Dynamics

To investigate the dynamics of imaginal disc cell membranes, we expressed GFP linked to glycophosphatidylinositol (gpi) in different subsets of the imaginal disc using the gal4/UAS system (Brand and Perrimon, 1993). Gpi anchors target proteins to the outer leaflet of the plasma membrane. Figures 1A, 1C, and 1D show confocal sections of living wing imaginal discs that express GFPgpi in the posterior compartment under the control of the *engal4* driver (the pattern of expression generated by *engal4* is diagrammed in Figure 1B). In the cells that express it, GFPgpi localizes predominantly to the basolateral membrane (Figures 1A and 1C). Strikingly, GFPgpi is also present in punctate structures in the nonexpressing anterior compartment (Figure 1C). The brightness of many of these particles is comparable to that of the plasma membrane of the expressing cells. To determine whether the fluorescence in putatively nonexpressing cells might be due either to low level background expression from the UAS:GFPgpi construct or to autofluorescence, we examined discs containing only the UAS:GFPgpi construct, but not the *engal4* driver, under the same imaging conditions used in Figure 1C. No fluorescent particles were detected anywhere in the wing imaginal disc (Figure 1D), ruling out artifacts due to autofluorescence and background expression. One interpretation of these results is that the basolateral membranes of disc cells can vesiculate and travel throughout the disc epithelium.

Markers of Both the Outer and Inner Membrane Leaflets Can Travel to Neighboring Cells

The brightness of the particulate GFP fluorescence throughout the nonexpressing region is close to that of the plasma membrane of expressing cells. Thus, it seems unlikely that partitioning of GFPgpi between basolateral membranes of adjacent cells could account for these observations; such a mechanism should produce generalized plasma membrane fluorescence whose brightness decreased rapidly with distance from the

[1] Correspondence: eaton@mpi-cbg.de

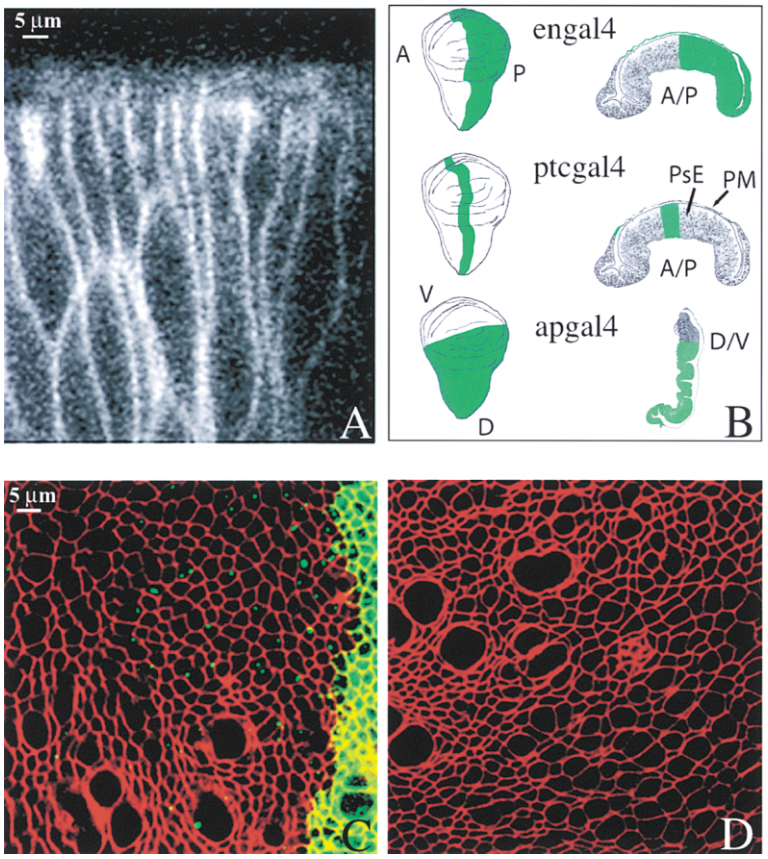

Figure 1. GFPgpi Localizes Basolaterally in Expressing Cells and in Punctate Structures in the Nonexpressing Region

(A) xz section through a living wing disc that expresses GFPgpi in the posterior compartment via *engal4*. Apical is up, basal is down. GFPgpi is localized basolaterally. The fuzzy fluorescence above the wing pouch cells is in the peripodial membrane.

(B) Schematic diagram of the regions of the wing disc where GFPgpi (green) is expressed by the driver lines indicated. Pictures on the left show an en face view of the wing disc. Pictures on the right show transverse sections through the wing pouch (for *engal4* and *ptcgal4)* and a longitudinal section (for *apgal4*). Imaginal discs consist of a folded sac of epithelial cells whose apical sides face the lumen. The cells of the peripodial membrane (PM) are much thinner and flatter than those of the pseudostratified epithelium (PsE). Note that the peripodial membrane expresses GFPgpi in *engal4* discs but not in *ptcgal4* or *apgal4* discs.

(C) xy section through a living disc expressing GFPgpi in the posterior compartment under the control of *engal4*. GFPgpi (green) localizes to the basolateral membrane of the posterior cells and in punctate structures in the anterior non-GFP-expressing cells. Cell boundaries are stained red by FM4-64.

(D) xy section of a disc containing the UAS-GFPgpi expression construct, but no GAL4 driver. No GFP fluorescence is detected under identical imaging conditions.

producing cells. Nevertheless, if mechanisms existed to extract GFPgpi from the membrane and maintain it in an aggregated state over large distances, they might produce the results we see. If the fluorescent particles in nonexpressing cells were produced by partitioning of GFPgpi from the membrane, then a fluorescent marker localized to the intracellular lipid leaflet should not be able to generate such particles. To ask whether this was so, we examined the distribution of a CFP-Rho GTPase fusion protein. Figure 2A shows that CFP-Rho localizes to the basolateral membrane in the cells that express it. Interestingly, we observed that CFP-Rho, like GFPgpi, is found in particulate structures throughout the nonexpressing region. Because markers of both the extracellular and cytoplasmic faces of the membrane can be found in particles throughout the nonexpressing region, it seems likely that these particles consist of complete membrane "exovesicles" derived from distant cells. We have called these exovesicles "argosomes" because of their ability to travel.

We have also examined the distribution of a second marker of the cytoplasmic face of the membrane: myristoylated GFP (mGFP). Like CFP-Rho, mGFP localizes to basolateral membranes; however, it generates only very few particles in the nonexpressing area (Figure 2B). The fact that CFP-Rho and myristoylated GFP are incorporated into argosomes with different efficiencies suggests that the protein composition of argosomes is nonrandom and that mechanisms may exist to specifically sort proteins into these membrane domains. Furthermore, the absence of significant numbers of labeled argosomes when mGFP is used to mark basolateral membranes confirms that low level activity of the GAL4 driver does not produce particulate fluorescence in putatively nonexpressing cells.

Argosomes Consist Mainly of Membrane

To investigate whether cytoplasm from the producing cells was carried in argosomes, we examined the distribution of a cytoplasmic form of GFP. We were unable to detect fluorescence in nonexpressing cells under these circumstances (Figure 2C). This suggests that argosomes have a high surface area to volume ratio, consisting predominantly of membrane and incorporating very little cytoplasm.

Argosomes Reside in an Endocytic Compartment

To determine whether argosomes are present inside or outside of cells, we closely examined GFPgpi-expressing discs that had also been labeled with FM4-64, a dye that fluoresces red upon insertion into membranes. When FM4-64 is applied extracellularly, it first inserts into the plasma membrane. Subsequently, as endocytosis proceeds, it is incorporated into endocytic vesicles and endosomes as well. We expected that the intracellular versus extracellular location of argosomes should often be immediately obvious upon comparison with cell outlines. In more ambiguous cases where argosomes lie near cell boundaries, we expected that an extracellular particle would immediately bind FM4-64 resulting in a bright red spot; in contrast, if argosomes were intracellular, they should be labeled only with green fluorescence

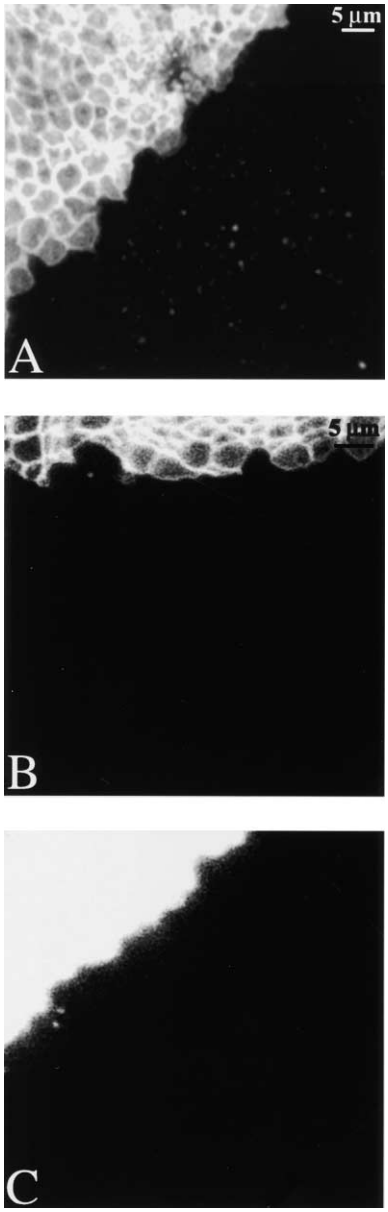

Figure 2. Fluorescent Particles in Nonexpressing Cells Consist of Complete Membrane Bilayers

(A)–(C) show discs expressing different GFP fusion constructs in the dorsal compartment under the control of the *apgal4*driver. Dorsal is up and ventral down.

(A) CFP-Rho (which localizes to the inner membrane leaflet) is found on the basolateral membrane of expressing cells and in punctate structures in the ventral nonexpressing area.

(B) Myristoylated GFP (another marker of the inner membrane leaflet) localizes to the basolateral membrane of the dorsal expressing cells but only in a very few particles in the nonexpressing area under the same imaging conditions.

(C) Very little cytoplasmic GFP is detected in the nonexpressing area under the same imaging conditions.

until they are endocytosed by another cell or fuse with a newly formed endocytic vesicle. We looked at living GFPgpi-expressing imaginal discs as soon as possible (10 min) after the addition of FM4-64, and at later time points between 1 and 3 hr after addition of FM4-64.

Figure 3 shows single confocal sections approximately 3 μm beneath the apical surface of the disc epithelium. Observation of the FM4-64-labeled cell boundaries shows that most argosomes are localized intracellularly. Within 10 min of FM4-64 addition (Figures 3A–3C), only a few (3/40) argosomes colocalize with FM4-64. Those that do are unambiguously intracellular and must represent a recent endocytic event (indicated by arrows in Figures 3A–3C). After longer incubations with FM4-64, increasing numbers of argosomes colocalize with the dye, although we do not observe total colocalization, even after many hours. In the example shown in Figures 3D–3F, 7 out of 19 argosomes are labeled by FM4-64. These data show that argosomes are intracellular, that a fraction of them are present in an early endocytic compartment, and that others remain inaccessible to endocytic markers over a long period. These data do not rule out the presence of smaller, dimmer argosomes outside of cells that are undetectable by these methods. It is also difficult to resolve whether argosomes that appear to lie on the cell boundary are inside or outside of the cell.

Argosomes Are Present in Structures that Can Move Rapidly and Generate Smaller Fragments

To study the movements of argosomes within cells, we collected a series of time-lapse images from GFPgpi-expressing discs. Some structures appeared relatively static (asterisk); others, often characterized by their tubular shape, moved rapidly in the plane of the epithelium (see Supplemental Movie 1 [available at http://www.cell.com/cgi/content/full/106/5/633/DC1] and Figure 4A). The example indicated by arrowheads in Figure 4A moves at 0.33 μm per second (see the linked movie for additional examples of moving tubular structures). Movement was also apparent along the apical-basal (AB) axis in folded regions of the disc where the AB axis of the epithelium lay parallel to the coverslip (data not shown). Some argosome-containing structures were observed to generate smaller labeled particles. In the example shown in Figure 4B, the daughter particle moves away at 0.14 μm/sec. In Supplemental Movie 2 (see URL above), it is apparent that the large GFP-labeled structure gives rise to multiple daughter particles, some of which appear tubular in shape and travel along the same "track." These data indicate that the endocytic compartment that contains argosomes can move at speeds that are broadly consistent with those of cellular motors. The fragmentation that we observe further suggests that at least some of these endosomes accumulate multiple argosomes, which can be directed along different cellular routes.

Models for Argosome Production

At least two possible models for the generation and movement of argosomes are consistent with our data, and these are outlined in Figure 4 (see also the discussion, where these models are described in more detail). In the first model, argosomes resemble the exosomes produced by cells of the hematopoeitic lineage (Denzer et al., 2000a). In this case, budding within an endosome generates a multivesicular endosome that is capable of fusing with the plasma membrane and releasing its internal vesicles. The second model involves the direct

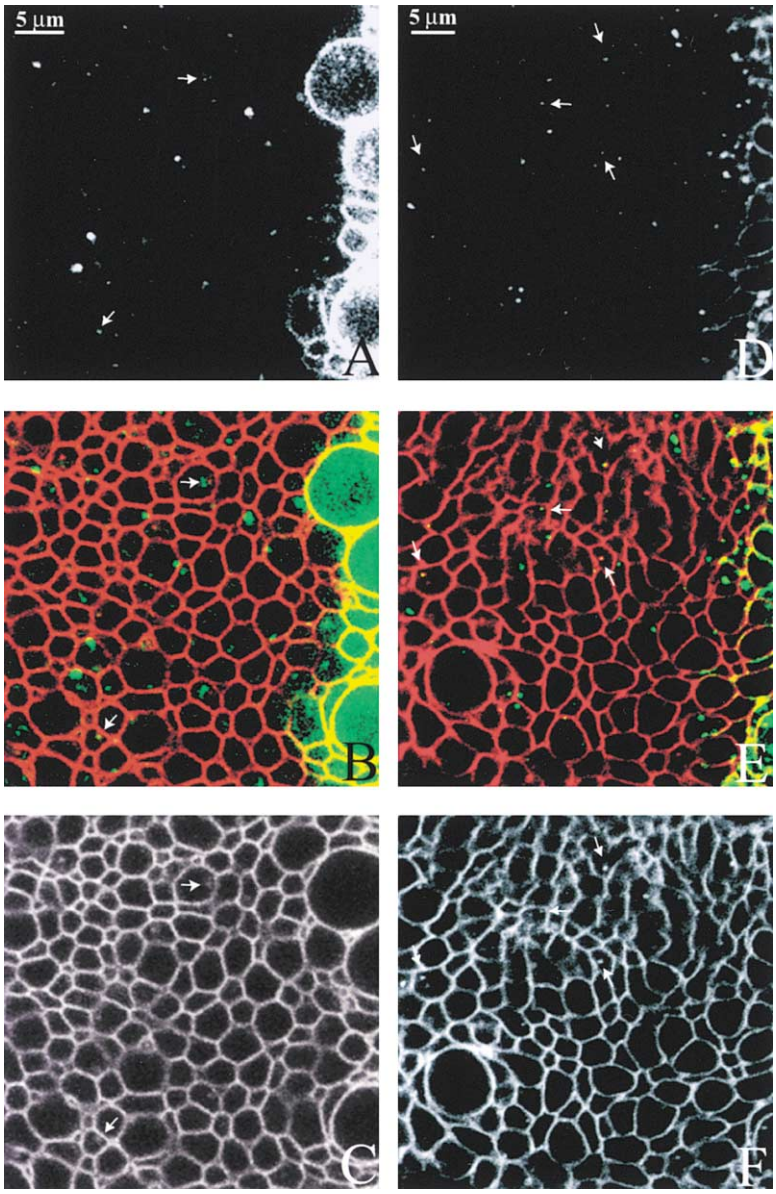

Figure 3. Argosomes Are Present in the Endocytic Compartment

(A–C) A live *engal4;UASGFPgpi* imaginal disc after ten minutes in the presence of FM4-64 (red). The argosomes (green) in the nonexpressing area are mainly located inside the cells. Some of the argosomes colocalize with newly formed endocytic structures, which label with FM4-64 (arrows).

(D–F) A live *engal4;UASGFPgpi* imaginal disc after 1 1/2 hr in FM4-64. Many, but not all, argosomes colocalize with FM4-64-labeled endosomes (arrows indicate colocalization).

internalisation of part of one cell by its immediate neighbor. This process is reminiscent of the endocytosis of transmembrane ligands observed for Boss/Sevenless (Cagan et al., 1992) and Notch/Delta signaling (Klueg and Muskavitch, 1999), and also shares features with the mechanism used by *Listeria* to spread through sheets of MDCK epithelial cells (Robbins et al., 1999). Both mechanisms produce intracellular membranous exovesicles with the same topology. Note that in each case the extracellular leaflet of the argosome, which potentially contains membrane-bound morphogens, faces the extracellular leaflet of the plasma membrane of the receiving cell and would therefore be capable of properly contacting receptor molecules.

Argosomes Are Produced by Many Different Regions of the Disc

Morphogens are generated by specific subsets of imaginal disc cells. To ask which subsets of cells within the disc are capable of generating argosomes, and how these particles are distributed, we expressed GFPgpi in a variety of different patterns and quantified the argosomes present at different distances from expressing cells. The expression patterns of the different drivers are shown in Figure 1B. We determined the total number of labeled argosomes in grids of 4 by 21 cells at increasing distances from expressing cells. Imaginal disc cells are much taller along their apical-basal axis than they are wide, and argosomes are distributed over their entire apical-basal length. We therefore summed all the argosomes present in a series of confocal sections beginning just below the apical surface and proceeding basally to a depth of 15 μm.

We first analyzed argosome distribution in the posterior compartment when GFPgpi was expressed under the control of the *ptcgal4* promoter along the anterior-posterior (AP) compartment boundary (Figure 5A, purple bars). GFPgpi-labeled argosomes were most abundant

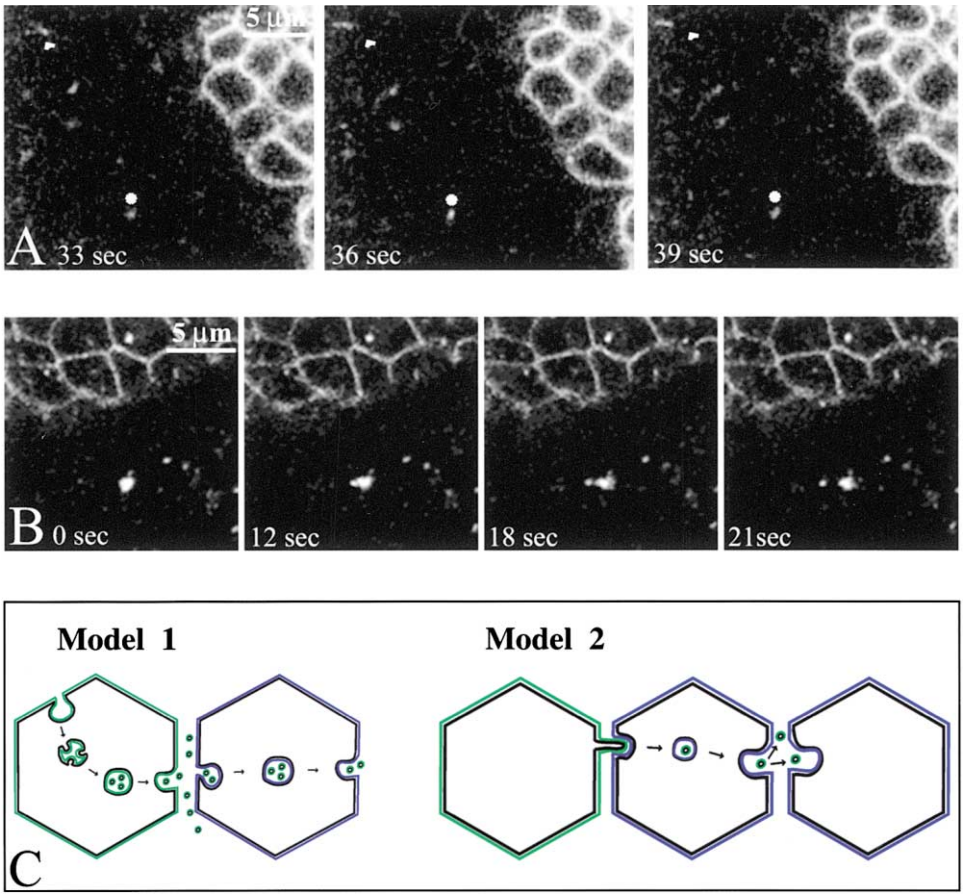

Figure 4. Argosome-Containing Endosomes Move Rapidly and Generate Smaller Fragments

(A) Discs expressing GFPgpi in the posterior compartment were imaged by time lapse confocal microscopy. Three consecutive frames are shown, separated by 3 s intervals. The arrowhead is positioned identically in all three frames and the particle it indicates moves at 0.33 μm per second.

(B) Four sequential frames show a large GFPgpi-labeled particle giving rise to a smaller daughter particle. The detached particle moves away with a speed of 0.14 μm per second.

(C) Two models for the generation of argosomes. In model 1, argosomes are generated from multivesicular endosomes, much like exosomes. In model 2, argosomes are generated by trans-endocytosis.

near the GFPgpi-producing cells. There were, on average, 161 labeled argosomes in the first grid of 4 by 21 cells (about 2 labeled argosomes per cell) and this number decreased by more than half over 12 to 16 cells. This distribution suggests that argosomes produced along the anterior side of the compartment boundary can traverse the boundary and travel through the posterior compartment.

We observed a similar gradient of GFPgpi-labeled argosomes in the anterior compartment when GFPgpi was produced in the posterior compartment under the control of the *engal4* promoter. In this case, an average of 266 labeled argosomes were found in the first grid of 4 by 21 cells (approximately three labeled argosomes per cell). This number decreased by approximately 50% over 12–16 cells (Figure 5A, aquamarine bars). These data show that argosomes produced in the posterior compartment can cross the compartment boundary and move through anterior tissue. The distribution of labeled argosomes was somewhat more variable when GFPgpi was driven by *engal4* rather than *ptcgal4* (see error bars). This is probably due to the spatial organization of the posterior compartment in which *engal4* is active. The posterior compartment comprises about half of the pseudostratified cells of the disc proper, along with much of the overlying peripodial membrane (see Figure 1B). In theory, labeled argosomes might be produced by cells of the peripodial membrane and transferred vertically to those of the pseudostratified epithelium. Furthermore, labeled argosomes might also enter the pseudostratified epithelium where it contacts the peripodial membrane at the edge of the wing pouch. Indeed, in some discs, we observed an increase in the number of labeled argosomes in this region. Nevertheless, the fact that labeled argosomes are most abundant near the AP compartment boundary in the wing pouch suggests that many argosomes are moving laterally from the posterior into the anterior compartment.

Taken together, these data show that argosomes can be generated by both anterior and posterior compartment cells and can undergo net movement away from the source in both anterior and posterior directions. This

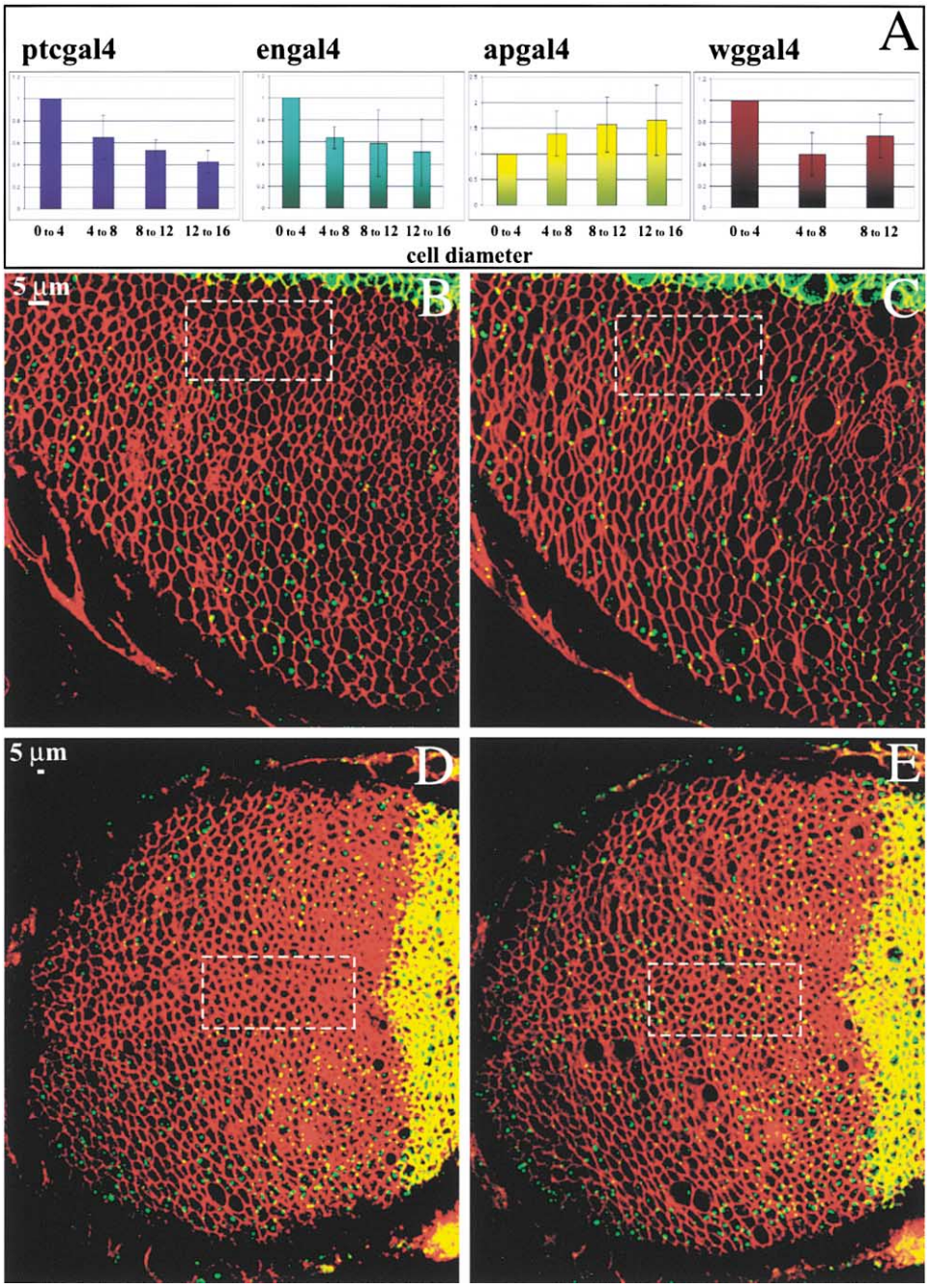

Figure 5. Argosomes Are Produced by Cells throughout the Disc

(A) Distribution of argosomes produced by different regions of the disc. GFPgpi was expressed along the AP compartment boundary with *ptcgal4* (purple), in the posterior compartment with *engal4* (aquamarine), in the dorsal compartment with *apgal4* (yellow), or in the *wingless*-expressing cells with *wggal4* (red). Fifteen confocal sections were collected every micron beginning just below the apical surface. The nonexpressing region of the disc (the posterior compartment in the case of *ptcgal4*) was divided into grids of 4 by 21 cells, and the total number of argosomes in each grid was counted. The relative abundance of argosomes in the different grids was calculated for each disc and then averaged. The number of discs averaged was 6 (for *engal4*), 3 (for *ptcgal4*), 3 (for *apgal4*), and 5 (for *wggal4*).

(B) A single confocal section 1 micron below the apical surface of a living disc expressing GFPgpi under the control of *apgal4*. Cell boundaries are stained red by FM4-64. Argosomes are less abundant in a region about 4 cells wide adjacent to the D/V boundary. These cells comprise the ventral Wingless-expressing cells.

(C) A more basolateral section of the same region of the same disc as in (B). Argosomes are present in cells adjacent to the DV boundary.

(D) A single confocal section 1 micron below the apical surface from a living disc expressing GFPgpi in the posterior compartment under the control of *engal4*. Cell boundaries are stained red by FM4-64. Argosomes are less abundant near the DV boundary.

(E) A more basolateral section of the same region of the same disc as in (D). Argosomes are now detected easily at the DV boundary.

is further supported by the observation that labeled argosomes are present throughout the wing pouch when GFPgpi is expressed on its lateral margins with *brinkergal4* (data not shown).

Argosome Trafficking Is Actively Regulated along the Dorsal-Ventral Axis

To characterize argosome movement along the dorsal ventral (DV) axis, we expressed GFPgpi in the dorsal compartment under the control of the *apterous* promoter and monitored argosome distribution in the ventral compartment. Interestingly, we found that the first four rows of cells nearest to the expressing cells had fewer argosomes than those more distant (an average of 218 in the first grid of 4 by 21 cells as compared with 294 elsewhere) (Figure 5A, yellow bars). This effect was stronger in the apical-most region (indicated by the outlined rectangles in Figures 5B and 5C); in the most apical 4 microns of the disc shown in Figure 5B, only 72 argosomes were present in the first four rows of cells, as compared to 159 in the next four rows of cells. Although many discs have a slight indentation in the apical surface at the dorsal/ventral boundary, we used FM4-64 staining to confirm that only the flattest discs were used for quantification, and that equivalent regions of all cells were included in the quantifications. Therefore, we do not think that the topology of the disc accounts for these differences in argosome abundance.

To see whether the reduced number of argosomes in cells near the DV boundary was an autonomous property of these cells or whether it depended on the expression pattern generated by apgal4, we examined more closely the distribution of argosomes in engal4; GFPgpi discs. We observed an identical reduction in argosome number in cells straddling the DV boundary that was most apparent apically (outlined rectangles in Figures 5D and 5E). These data suggest that cells near the DV boundary traffic argosomes differently; these cells may internalize argosomes less efficiently, or they may degrade or recycle argosomes more rapidly than their neighbors.

Wg-Expressing Cells Produce Argosomes

The cells along the DV boundary that accumulate apical argosomes less efficiently comprise the *wingless* expression domain, along with approximately two additional rows of cells. To test whether *wingless*-expressing cells were nevertheless capable of producing argosomes, we examined discs expressing GFPgpi under the control of *wggal4* (Figure 5A, red bars). In these discs, we observed argosomes that were most abundant near the *wingless*-expressing domain straddling the DV boundary (an average of 154 in the first grid of 4 by 21 cells, or 1.8 per cell). The next grid of cells contained only 77 argosomes on average. Argosome abundance increased again at greater distances from the DV boundary, perhaps reflecting argosomes produced by the *wingless*-expressing cells of the hinge region, which surrounds the wing pouch. These data show that the cells that produce Wingless also produce argosomes.

The number of labeled argosomes per cell varied from disc to disc and depended on the line used to drive GFPgpi expression. In general, we observed more labeled argosomes when the level of GFPgpi on the plasma membrane of producing cells was high—for example, adding copies of the GFPgpi expression construct or raising the temperature of growth (thus increasing GAL4-dependent transcription) allowed us to observe more argosomes, even when the same driver was used (data not shown). We conclude that there is a threshold of brightness below which we cannot observe argosomes. Although we detect fewer argosomes overall when expression is driven by *wggal4* or *ptcgal4*, compared with *engal4* or *apgal4*, this may reflect the level of GFPgpi expression rather than any intrinsic difference in the ability of these cells to make argosomes.

The Argosome Gradient Reforms Rapidly after Photobleaching

The speeds with which different morphogen gradients are established have been reported to be between 15–60 min (Strigini and Cohen, 2000) and 3 hr (Entchev et al., 2000; Teleman and Cohen, 2000). If argosomes act as vehicles for the spread of morphogens, the rate at which argosomes spread through the disc epithelium ought to reflect this. To address this question, we used photobleaching to render preexisting argosomes invisible throughout the nonexpressing region (the photobleached area is shown in black in Figure 6A). We then monitored the spread of newly formed argosomes through the first 16 cell rows adjacent to GFPgpi-producing cells (the outlined rectangle in Figure 5A). To ensure that those argosomes we counted represented newly emerged argosomes rather than an older, incompletely bleached population, we counted only those particles that colocalized with FM4-64. Since movement of argosomes through the epithelium must involve either endocytosis or exposure to the extacellular milieu, any argosomes that do not label with the dye almost certainly represent those present before photobleaching. Almost all the argosomes that emerged during recovery colocalized with FM4-64 (Figure 6D), suggesting that they had emerged since photobleaching.

Very few argosomes were present at 4 min after the beginning of photobleaching (Figure 6B). However, we began to observe significant recovery of argosomes in the first four rows of cells within 26 min (Figure 6E). Between 26 min and 3 hr, their distribution became broader and argosomes were found up to 16 cells away from the producing cells (Figures 6C and 6E). These data show that argosomes are released by GFPgpi-producing cells and spread through the adjacent epithelium at rates that are roughly consistent with speeds at which morphogen gradients form.

Argosomes Colocalize with wg-Containing Vesicles

Wingless protein can be found on the basolateral membranes of the cells that synthesize it. To see whether argosomes derived from these basolateral membranes might contain Wingless, we looked for colocalization between Wingless and GFPgpi-labeled argosomes. We fixed discs that expressed GFPgpi under the control of either *wingless* or *apterous*, mildly permeabilized them, and stained them with an antibody to Wingless. Fixation and permeabilization drastically reduces the number of

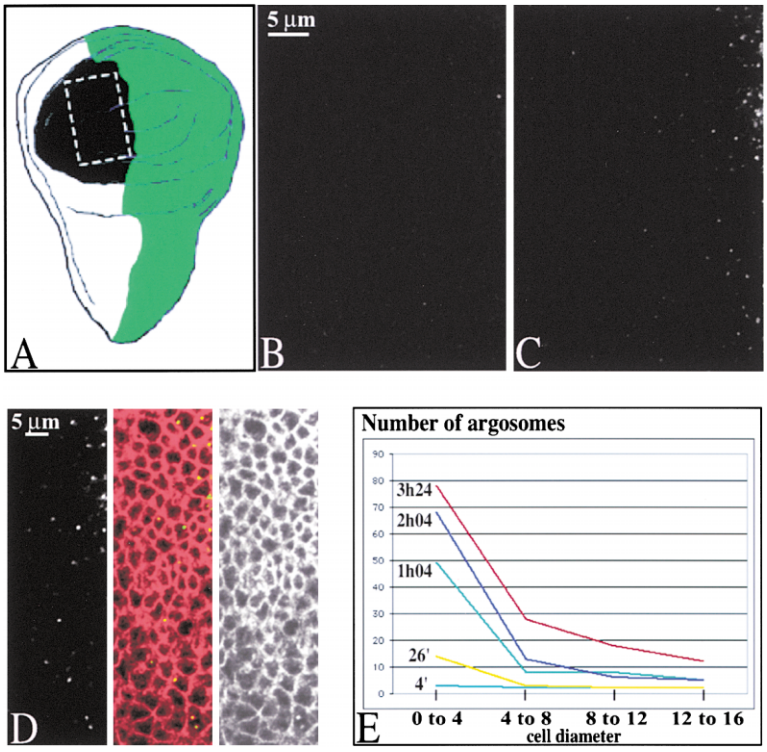

Figure 6. Recovery of Argosome Formation after Photobleaching

(A) The anterior nonexpressing area of an *engal4:UAS:GFPgpi* wing imaginal disc was photobleached with the 488 nm laser line at full power. The black region indicates the photbleached area. Immediately and at various intervals thereafter, the disc was reimaged at normal laser power over a total vertical range of 15 microns in the region outlined by the rectangle.

(B) Projection of 15 confocal sections collected 4 min after the beginning of photobleaching (the length of time required for photobleaching and storage of the resulting image). The GFP-gpi-producing cells lie just to the right of the region depicted.

(C) Projection of 15 confocal sections from the same region as in (B) collected 2 hr and 4 min after the beginning of photobleaching.

(D) A single confocal section showing both FM4-64 staining (red) and GFPgpi (green), along with an overlay of the two channels, 2 hr after photobleaching. In this panel, only one argosome fails to colocalize with FM4-64.

(E) Time course of recovery of argosomes at different distances from GFPgpi-producing cells. Colored lines show the number of argosomes per grid of 4 by 21 cells progressively farther from the producing cells at different times after photobleaching.

detectable argosomes. Nevertheless, we were able to detect significant colocalization of the remaining argosomes with Wingless (arrows in Figures 7A and 7B). When GFPgpi was expressed with *apgal4*, a fairly strong driver, we observed up to 50% colocalization, i.e., half of the Wingless-positive vesicles were also positive for GFPgpi (Figure 7A). Since only half of the argosomes derived from Wingless-expressing cells will be marked by GFPgpi when its expression is driven by *apterous*, 50% represents very significant colocalization. *Wggal4* drives the expression of GFPgpi to a lower level than *apgal4*, and we detect fewer argosomes under these circumstances. Nevertheless, up to 50% of Wingless-positive vesicles are also labeled with GFP in these discs (Figure 7B). Since we see fewer argosomes after fixation and permeabilization, the true extent of colocalization has probably been underestimated. These data show that, in many cases, Wingless is present in the same structures as membrane derived from Wingless-producing cells. This suggests that argosomes may provide a vehicle for the movement of the Wingless protein.

Heparin Sulfate Proteoglycans Are Required for Wingless Localization on Argosomes

If argosomes mediate the movement of Wingless through the disc epithelium, then the ability of Wingless to associate with membranes would be essential for its long range distribution. Since Wingless is thought to associate with membranes via HSPGs, we tested whether treating discs with different heparinases could alter the distribution of Wingless. We treated discs with either heparinase I or heparinase III at concentrations known to perturb Wingless signaling in embryos (Binari et al., 1997). Under these conditions, Wingless protein was strongly depleted both from Wingless-expressing cells and from the surrounding tissue (compare Figures 8A and 8B). Normally, Wingless-producing cells contain Wingless both on their basolateral membranes (Figure 8D), and in bright cell-internal spots (Figures 8C and 8D) that are especially abundant apically. Consistent with the phenotype of *sulfateless* clones, Wingless was undetectable on the plasma membrane after incubation with either heparinase I or III (compare Figures 8D and 8F). Strikingly, we also observed a strong reduction in the number of cell-internal Wingless spots (compare Figures 8C and 8E). These data show that HSPGs must be present in order for Wingless to accumulate normally within the cells that produce it. EM studies have shown that most Wingless inside producing cells is contained within multivesicular endosomes (van den Heuvel et al., 1989). Therefore, one explanation for these observations is that, in producing cells, Wingless is endocytosed and accumulates via a mechanism that depends on binding to HSPGs. Alternatively, HSPGs might be required for Wingless biosynthesis or stability.

Wingless was almost undetectable in cells on either side of the Wingless stripe after treatment with heparinase I, and a slightly weaker effect was observed after incubation with heparinase III (Figures 8A and 8B). To quantify these differences, we enumerated Wingless particles present within 20 μm on either side of the Wingless stripe for between 7 and 9 discs (see legend to Figure 8). In discs incubated in tissue culture medium, we detect on average 277 Wingless particles. In contrast, after incubation with heparinase I or III, we counted only 7 and 56 Wingless particles, respectively, in the same area. The absence of Wingless protein in nonex-

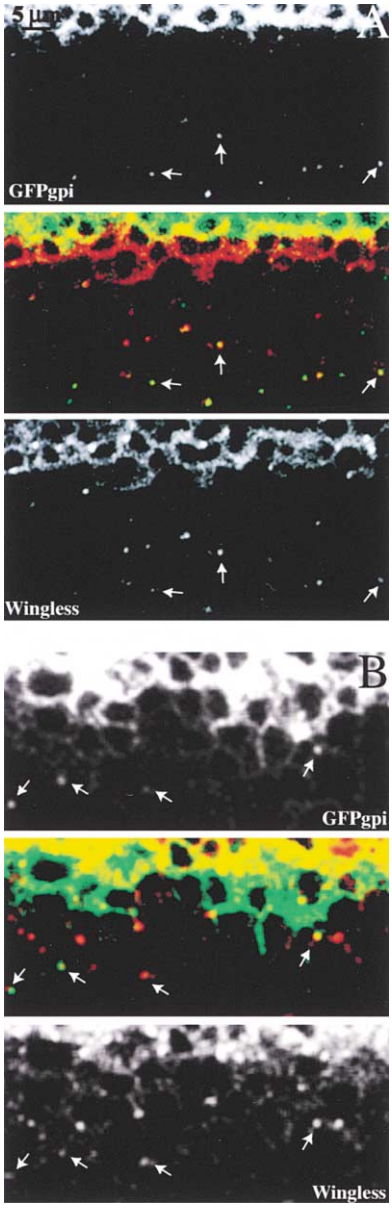

Figure 7. Wingless-Expressing Cells Form Argosomes that Colocalize with Wingless in Receiving Cells

(A) Discs that expressed GFPgpi under the control of *apgal4* were fixed, permeabilized, and stained with an antibody to Wingless. Wingless (red) colocalizes with argosomes (green) produced by *apterous*-expressing cells.

(B) Discs that expressed GFPgpi under the control of *wggal4* were fixed, permeabilized, and stained with an antibody to Wingless. Wingless (red) colocalizes with argosomes (green) produced by Wingless-expressing cells.

pressing tissue may be a secondary consequence of the failure of Wingless to accumulate normally in the cells that produce it. Alternatively, HSPGs may be required independently in receiving tissue for Wingless accumulation. In either case, these data suggest that membrane association via HSPGs plays an important role in the movement of Wingless through the disc epithelium.

To ask whether the argosome production was perturbed by removal of HSPGs, we examined argosome distribution in heparinase I- and heparinase III-treated discs. No alteration was observed (Figure 8G). These data suggest that argosomes are produced whether or not Wingless is able to associate with them. This idea is consistent with the observation that cells in many different regions of the disc make argosomes. Argosomes may represent a widely utilized transport mechanism that is exploited by different cells for different purposes.

Discussion

Argosomes Are Basolateral Membrane-Derived Particles that Spread through the Disc Epithelium

We have identified a novel cell biological mechanism whereby fragments of basolateral membranes are transported over large distances through the disc epithelium. When basolateral membrane-associated GFPs are expressed in different subsets of the wing disc, fluorescence is observed not only on the plasma membrane of expressing cells, but also within endosomes throughout the nonexpressing region. We have called these fluorescent particles "argosomes."

The release and graded dispersal of morphogens such as Wingless form the basis for key patterning events in many different tissues. Despite its ability to travel many cell diameters away from the cells that produce it, the Wingless protein has a strong affinity for cell membranes (Bradley and Brown, 1990; Papkoff and Schryver, 1990; Reichsman et al., 1996). Our observations suggest that Wingless can move through the disc epithelium on argosomes. First, Wingless-producing cells make argosomes that are derived from the basolateral membrane, which contains high levels of the Wingless protein. Second, Wingless in receiving cells colocalizes with argosomes derived from cells that synthesize Wingless. Finally, the rate at which argosomes spread through the disc epithelium is broadly consistent with the rate at which Wingless travels.

The Hedgehog protein binds to membranes via cholesterol and palmitate (Porter et al., 1996; Pepinsky et al., 1998) and is another obvious candidate for an argosome passenger. We are currently developing the tools to address this intriguing possibility.

Formation of Membrane Exovesicles Occurs in Many Different Cell Types

The release of membranous exovesicles forms the basis for signaling events in many different cell types. The uptake of entire regions of the plasma membrane has been considered as a mechanism for the endocytosis of transmembrane ligands (Cagan et al., 1992; Klueg et al., 1998; Klueg and Muskavitch, 1999; Parks et al., 2000). Uptake of parts of neighboring cells, or "trans-endocytosis" certainly seems to occur between MDCK epithelial cells, a process that is exploited by *Listeria* as it spreads through the epithelium (Robbins et al., 1999). Trans-endocytosis might similarly account for the initial formation of argosomes (Figure 4C, model 2); their long-range movement would require the subsequent release of these endocytosed exovesicles.

An alternative possibility (depicted in Figure 4C, model

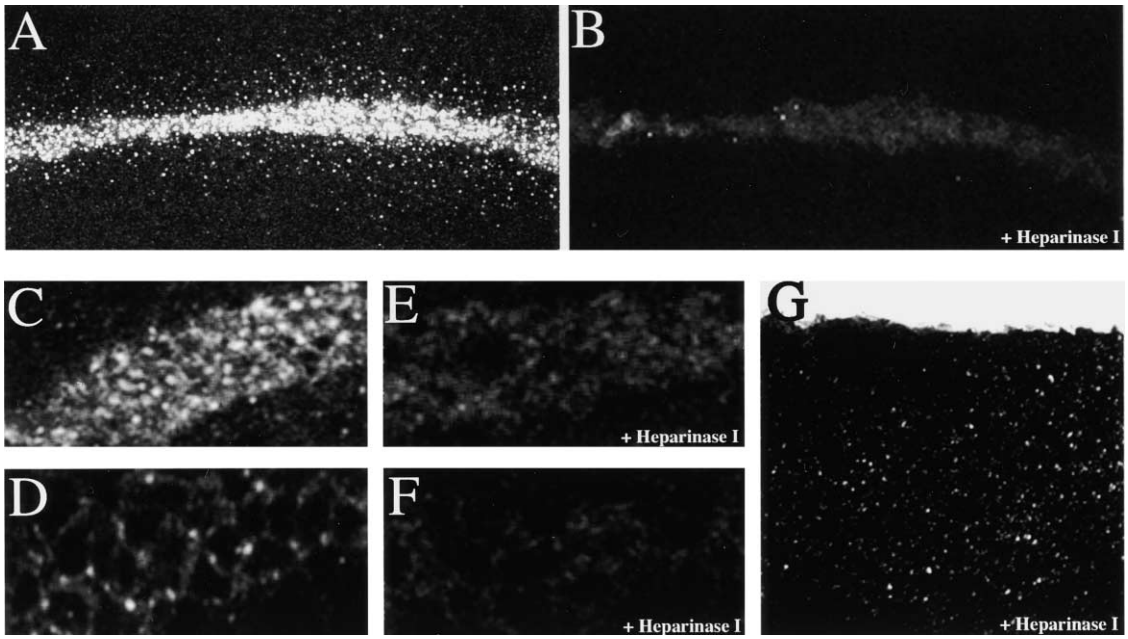

Figure 8. Wingless Protein Is Depleted after Heparinase Treatment

(A)–(E) show discs stained with Wingless antibody.

(A) Projection of 15 confocal sections of a mock-treated disc. Wingless protein is found at high levels in Wingless-expressing cells and in punctate structures outside of the expression domain.

(B) Projection of 15 confocal sections of a disc treated for 3 hr with heparinase I. Wingless protein is depleted from both Wingless-expressing cells and the surrounding tissue. Wingless particles present within 20 μm on either side of the Wingless stripe were enumerated. The number of particles was then normalized to the length of the Wingless stripe in each disc. Eight mock-treated discs had 275, 449, 8, 301, 40, 148, 493, and 501 particles per 100 μm. Seven heparinase I-treated discs had 18, 8, 1, 4, 13, 4, and 0 particles per 100 μm. Nine heparinase III-treated discs had 35, 42, 13, 4, 21, 168, 206, 10, and 9 particles per 100 μm.

(C) A single confocal section of a mock-treated disc taken 1 μm below the apical surface of the disc epithelial cells. Wingless is most obviously present within punctate structures.

(D) A single confocal section of a mock-treated disc taken 6 μm below the apical surface of the disc epithelial cells. Wingless can be seen on the basolateral membrane, as well as in punctate structures.

(E) A single confocal section of a heparinase I-treated disc taken 1 μm below the apical surface of the disc epithelial cells. Wingless is much less abundant in apical punctate structures.

(F) A single confocal section of a heparinase I-treated disc taken 6 μm below the apical surface of the disc epithelial cells. Wingless is much less abundant on the basolateral membrane.

(G) Argosomes produced by a heparinase I-treated disc.

1) is that argosomes are formed by a mechanism similar to that of exosomes, which are produced by cells of the hematopoeitic lineage (reviewed in Denzer et al., 2000a). Exosomes are formed within endosomes as specific membrane proteins and lipids are recruited into inwardly budding vesicles. When the limiting membrane of the multivesicular endosome fuses with the plasma membrane, exosomes are released into the extracellular space. Because protein sorting into exosomes is tightly regulated, it allows different cells to produce exosomes with highly specific functions and target cell specificities. Cytolytic T cells produce exosomes that deliver killing reagents specifically to their targets (Peters et al., 1989, 1990). Exosomes derived from antigen-presenting cells carry peptide-MHC molecules and are capable of activating specific subsets of T cells in vitro (Raposo et al., 1996; Zitvogel et al., 1998).

Although it is possible that the mechanism that gives rise to argosomes might share features with exosome production, argosomes have other properties that make them completely unique. While exosomes can bind to the membranes of target cells (Denzer et al., 2000a), they have never been observed to be endocytosed, much less to travel through tissue. It is to be expected that these novel functions, peculiar to argosomes, will depend on their specific protein or lipid composition, which must differ from that of exosomes.

Argosomes and the Spread of Wingless

The membrane affinity of Wingless is essential for its distribution and function; Wingless binds to membranes via heparan sulfate proteoglycans, and mutations that disrupt their synthesis interfere with Wingless signaling (Binari et al., 1997; Haerry et al., 1997; Lin and Perrimon, 1999, 2000; Tsuda et al., 1999; Baeg et al., 2001). Despite the central importance of HSPGs to Wingless signaling, the cell biological mechanisms they control are not completely understood. We would propose that one function for the interaction of Wingless with HSPGs might be to allow the incorporation of Wingless into argosomes. Such a model would predict that Wingless is endocytosed via its interaction with HSPGs shortly after secretion. As endosomes undergo internal budding, the Wingless/HSPG complex is incorporated onto these internal

vesicles and ends up in multivesicular endosomes. Fusion of the limiting membrane of the multivesicular endosome with the plasma membrane results in the release of Wingless/HSPGs on membranous exovesicles. In support of such an idea, it has been known for some time that Wingless is localized not only on the plasma membranes of the cells that synthesize it, but in multivesicular endosomes within these cells (van den Heuvel et al., 1989). If argosomes were made by an exosome-like mechanism, this is precisely the subcellular localization that would be predicted for Wingless

Consistent with this model, we have shown that heparinase treatment of imaginal discs results in the failure of Wingless to accumulate within Wingless-producing cells. This depletion may occur as free Wingless is secreted and diffuses away, rather than being endocytosed and directed to multivesicular bodies via HSPGs. Of course, it is also possible that Wingless depletion after heparinase treatment reflects other roles for HSPGs in Wingless biosynthesis or stabilization.

In addition to depleting Wingless from producing cells, heparinase treatment strongly reduces the level of Wingless found on punctate structures in surrounding tissue. In contrast, heparinase does not reduce the number of argosomes found in this region. These data show that HSPGs are necessary for association of Wingless with argosomes in receiving tissue, and they suggest that failure to incorporate Wingless into argosomes in producing cells might account for its absence in the surrounding tissue. Nevertheless, these data cannot rule out a requirement for HSPGs in the receiving tissue itself.

Argosomes resemble exosomes in that their protein composition appears to be nonrandom. GFPgpi is incorporated efficiently into argosomes, as is gpi-linked horseradish peroxidase (V.G. and S.E., unpublished), however GFP that is linked to the membrane via a single myristoyl group is not. Gpi linkage is thought to target proteins to raft lipid microdomains; consistent with this, GFPgpi associates with rafts in imaginal disc membranes. (K. Brady and S.E., unpublished results). Raft domains play important roles in the sorting of membrane proteins, and it is intriguing to speculate that they may promote protein sorting into argosomes. In this context, the association of Wingless to the cell membrane via Dally-like—a gpi-linked HSPG—is especially suggestive. Dally-like might be expected to sort into argosomes via its gpi linkage, carrying Wingless with it. An inability to sort into membrane domains destined for argosome formation might explain the failure of Wingless to signal at long range in imaginal discs when fused to the transmembrane domain of Neurotactin (Zecca et al., 1996).

The potential for specific protein sorting and concentration in argosomes makes them an attractive vehicle for the spread of membrane bound morphogens like Wingless that act at long range; in theory, they could deliver concentrations of morphogen not attainable by diffusion through the extracellular space, or even restricted diffusion along the surfaces of epithelial cells. Furthermore, the possibilities for specific control of adhesiveness between argosomes and target cells could provide additional mechanisms for controlling signaling specificity or efficiency.

The Wingless protein is distributed in a gradient both intracellularly and extracellularly, and it has been proposed that Wingless spreads predominantly by extracellular diffusion along cell membranes (Strigini and Cohen, 2000; Baeg et al., 2001). In contrast, GFPgpi-labeled argosomes are detected predominantly within cells. What is the relationship between argosomes and the extracellular gradient of Wingless protein?

Despite the fact that we detect argosomes mainly inside cells, our data do not conclusively demonstrate that they move through cells by planar transcytosis rather than extracellularly. Based on our experience with different GFPgpi expression levels, there is a brightness threshold below which labeled argosomes are undetectable. It is clear that many of the structures we see inside cells accumulate multiple argosomes, because they are able to split and give rise to multiple labeled daughter particles. Single argosomes, or argosomes that were more dispersed might be too dim to detect. Thus, it is possible that more dispersed extracellular argosomes would not be bright enough to be visible. Accordingly, extracellular Wingless might be present on small extracellular argosomes. Follicular dendritic cells display exosomes on their surface that are derived from B-lymphocytes; it is clear that exosomes produced by one cell can become firmly attached to another (Denzer et al., 2000b). Another alternative is that some fraction of argosomes might transfer their cargo to the plasma membrane of receiving cells by fusing with them. Of course, a third possibility is that Wingless can move either on argosomes, or extracellularly, and that these two forms of dispersal are mechanistically unrelated.

Argosomes form part of a novel cell biological mechanism responsible for the spread of membrane fragments throughout the disc epithelium. The existence of this mechanism has striking implications for the transport of morphogens with high membrane affinity. In particular, the consistent association of Wingless with argosomes in receiving tissue and the prevention of this association by removal of HSPGs suggests that argosomes could be a potential mechanism for Wingless transport. The development of techniques that specifically disrupt argosome production or movement will be required to resolve this issue unambiguously.

Experimental Procedures

Mounting Live Discs for Microscopy

Wing imaginal discs were dissected from third instar larvae in Grace's or SF900 insect media (Sigma). Live imaginal discs were then transferred onto glass slides into drops of medium delimited by double-sided adhesive tape. These chambers were constructed by cutting a rectangular section out of a piece of tape; a small channel was cut in the tape in order to allow superfluous medium to escape when the cover slip was placed on top. After positioning the coverslip, the channel was sealed with vacuum grease to prevent evaporation of the medium. Imaginal discs were always oriented with the apical surface facing the cover slip. As an alternative method, we sometimes placed imaginal discs in Petri dishes that had been modified to allow visualization of samples in an inverted microscope (MatTek Corp., Ashland, MA). Imaginal discs were observed using either a Leica TCS SP2 or a Zeiss LSM 510 confocal microscope.

Collection of z Stacks for Argosome Quantification

We chose for quantification those imaginal discs that FM4-64 staining showed to be lying flat against the coverslip and which had no

major defects or damage. XY sections were collected every 1 micron starting just below the peripodial membrane until no argosomes were detected (about 15 microns below the apical surface). The nonexpressing region of the disc was divided into grids of 4 by 21 cells, and the total number of argosomes in each grid was counted for all the sections collected. All discs were imaged under identical laser power, contrast, and threshold conditions. We counted as argosomes only those spots whose brightness was at least 50% of that of the plasma membrane (determined using the plot profile feature of NIH image).

In cases where GFPgpi expression was driven by *wggal4*, the dorsal compartment was chosen for quantification because it appeared to be flatter than the ventral compartment. When quantifying the reduction in argosomes present at the DV boundary, we paid special attention to the slight groove that occurs there; we chose discs where it was not pronounced, and ensured that our sections included the apical regions of all cells in the field.

Adobe Photoshop and NIH Image were used for image processing.

Timelapse Imaging of Argosome Movement

The timelapses were performed in the more apical regions of the disc. Each frame was collected using line averaging and comprised 3.1 s. Consecutive images were collected with no delay between them such that they were separated by 3.1 s. NIH Image and Quicktime were used for image processing.

Staining Cell Membranes with FM4-64

Concentrated FM4-64 stock was prepared by dissolving FM4-64 powder (Molecular Probes, Eugene, OR) in PBS to a final concentration of 16 mM. Wing imaginal discs were transferred onto a glass chamber slide into a drop of medium that contained 9 μM FM4-64. Approximately 10 min were needed to seal the chamber, move to the microscope, find a suitable disc, and begin acquisition.

Photobleaching Conditions

The anterior nonexpressing area of an *engal4*;*UASGFPgpi* wing imaginal disc was photobleached with the 488 nm laser line at full power and open pinhole. After various periods of time, the disc was reimaged at lower 488 nm laser power over a total vertical range of 15 microns. The 598 laser was also used to detect the FM4-64 marker, which was not photobleached.

Heparinase Treatment

Wing imaginal discs were dissected from third instar larvae in Grace's insect media (Sigma) and then transferred in eppendorf tubes containing either 100 μl Grace's medium alone, or 100 μl Grace's medium and 0.5 mg/ml heparinase I or III. These levels of heparinase have been shown to cause Wingless loss-of-function phenotypes when injected into embryos (Binari et al., 1997). Imaginal discs were then incubated for 3 hr at room temperature, washed, and fixed with 4% PFA for 20 min. After fixation, the discs were either washed with PBS and mounted in Prolong Anti Fade (Molecular Probes) for argosome observation, or processed as described below for Wingless staining.

Immunological Methods

For imaginal discs that were to be stained with anti-Wingless antibody, we dissected larvae in Grace's medium and collected imaginal discs in eppendorf tubes at room temperature. Imaginal discs were fixed in 4% paraformaldehyde in PBS for 20 min and then permeabilized with 0.05% Triton X-100 in PBS (PBT) twice for 10 min. The imaginal discs were then blocked twice for 15 min in PBT, 1 mg/ml BSA, and 250 mM NaCl, then incubated overnight at 4°C with a 1:10 dilution anti-Wingless (Strigini and Cohen, 2000) in PBT and 1 mg/ml BSA. Then they were washed twice for 20 min with PBT and 1 mg/ml BSA and twice for 20 min with the blocking solution PBT , 1 mg/ml BSA, and 4% normal goat serum (NGS). The imaginal discs were then incubated for at least 2 hr in a 1:1000 dilution of Alexa 594-conjugated secondary antibody (Molecular Probes, Eugene, OR). The antibody was removed by washing twice for 15 min with PBT and twice for 15 min in PBS. Last, the imaginal discs were mounted with Prolong Anti Fade (Molecular Probes) and allowed to set for at least three hours before observation.

Fly Stocks

The UAS:CFP-Rho construct produces a protein in which CFP is fused to the C terminus of DrhoA. Antibodies to both GFP (Molecular Probes, Eugene, OR) and Rho (Santa Cruz) recognize a single band of the correct size on Western blots (data not shown).

The UAS:GFPgpi construct was made by fusing the signal sequence of rabbit lactase-phlorizin hydrolase (LPH) and the GPI attachment signal of lymphocyte function associated antigen 3 (LFA-3) to either side of GFP (Keller et al., 2001), and cloning the fusion construct into pUAST. The size of the protein on Western blots indicated that the transmembrane domain had been removed and replaced with GPI. Density gradient centrifugation showed that the fusion protein was membrane associated (data not shown).

UAS cytoplasmic GFP and UAS myristoylated GFP-containing flies are available from the Bloomington stock center, as are the *Apgal4*, *ptcgal4*, and *engal4* fly stocks. The *winglessgal4* driver line was a gift from Steve Cohen, and Tetsuya Tabata kindly provided the *brinkergal4* flies.

Acknowledgments

We thank Patrick Keller for providing the GFPgpi fusion construct and for lots of help with image processing. We thank Kai Simons for his invaluable advice and comments and Jens Rietdorf for assistance with the confocal microscope. We thank Stephanie Neutz for molecular cloning and Anne Marie Voie for performing injections of embryos. We are grateful to Steve Cohen and his lab for helpful discussions and for providing the Wingless antibody and many different fly stocks. We thank Steve Cohen, Marcos Gonzalez, Kai Simons, Elly Tanaka, and Marino Zerial for critically reading the manuscript. We especially benefited from discussing possible mechanisms of argosome dispersal with James H. Eaton.

Received March 19, 2001; revised August 1, 2001.

References

Baeg, G.H., Lin, X., Khare, N., Baumgartner, S., and Perrimon, N. (2001). Heparan sulfate proteoglycans are critical for the organization of the extracellular distribution of Wingless. Development *128*, 87–94.

Bellaiche, Y., The, I., and Perrimon, N. (1998). Tout-velu, a Drosophila homologue of the putative tumor supressor gene Ext-1, is required for the diffusion of the Hedgehog protein. Nature, in press.

Binari, R.C., Staveley, B.E., Johnson, W.A., Godavarti, R., Sasisekharan, R., and Manoukian, A.S. (1997). Genetic evidence that heparin-like glycosaminoglycans are involved in wingless signaling. Development *124*, 2623–2632.

Bradley, R.S., and Brown, A.M. (1990). The proto-oncogene int-1 encodes a secreted protein associated with the extracellular matrix. EMBO J. *9*, 1569–1575.

Brand, A.H., and Perrimon, N. (1993). Targeted gene expression as a means of altering cell fates and generating dominant phenotypes. Development *118*, 401–415.

Cadigan, K.M., Fish, M.P., Rulifson, E.J., and Nusse, R. (1998). Wingless repression of *Drosophila* frizzled 2 expression shapes the Wingless morphogen gradient in the wing. Cell *93*, 767–777.

Cagan, R.L., Kramer, H., Hart, A.C., and Zipursky, S.L. (1992). The bride of sevenless and sevenless interaction: internalization of a transmembrane ligand. Cell *69*, 393–399.

Chen, Y., and Struhl, G. (1996). Dual roles for patched in sequestering and transducing Hedgehog. Cell *87*, 553–563.

Christian, J.L. (2000). BMP, Wnt and Hedgehog signals: how far can they go? Curr. Opin. Cell Biol. *12*, 244–249.

Denzer, K., Kleijmeer, M.J., Heijnen, H.F., Stoorvogel, W., and Geuze, H.J. (2000a). Exosome: from internal vesicle of the multivesicular body to intercellular signaling device. J. Cell Sci. *113*, 3365–3374.

Denzer, K., van Eijk, M., Kleijmeer, M.J., Jakobson, E., de Groot, C.,

and Geuze, H.J. (2000b). Follicular dendritic cells carry MHC class II-expressing microvesicles at their surface. J. Immunol. *165*, 1259–1265.

Entchev, E.V., Schwabedissen, A., and Gonzalez-Gaitan, M. (2000). Gradient formation of the TGF-β homolog Dpp. Cell *103*, 981–991.

Haerry, T.E., Heslip, T.R., Marsh, J.L., and O'Connor, M.B. (1997). Defects in glucuronate biosynthesis disrupt Wingless signaling in Drosophila. Development *124*, 3055–3064.

Keller, P., Toomre, D., Diaz, E., White, J., and Simons, K. (2001). Multicolour imaging of post-Golgi sorting and trafficking in live cells. Nat. Cell Biol. *3*, 140–149.

Klueg, K.M., and Muskavitch, M.A. (1999). Ligand-receptor interactions and trans-endocytosis of Delta, Serrate and Notch: members of the Notch signalling pathway in Drosophila. J. Cell Sci. *112*, 3289–3297.

Klueg, K.M., Parody, T.R., and Muskavitch, M.A. (1998). Complex proteolytic processing acts on Delta, a transmembrane ligand for Notch, during Drosophila development. Mol. Biol. Cell *9*, 1709–1723.

Lawrence, P.A., and Struhl, G. (1996). Morphogens, compartments, and pattern: lessons from *Drosophila*? Cell *85*, 951–961.

Lin, X., and Perrimon, N. (1999). Dally cooperates with Drosophila Frizzled 2 to transduce Wingless signalling. Nature *400*, 281–284.

Lin, X., and Perrimon, N. (2000). Role of heparan sulfate proteoglycans in cell-cell signaling in Drosophila. Matrix Biol. *19*, 303–307.

Neumann, C., and Cohen, S. (1997). Morphogens and pattern formation. Bioessays *19*, 721–729.

Papkoff, J., and Schryver, B. (1990). Secreted int-1 protein is associated with the cell surface. Mol. Cell. Biol. *10*, 2723–2730.

Parks, A.L., Klueg, K.M., Stout, J.R., and Muskavitch, M.A. (2000). Ligand endocytosis drives receptor dissociation and activation in the Notch pathway. Development *127*, 1373–1385.

Pepinsky, R.B., Zeng, C., Wen, D., Rayhorn, P., Baker, D.P., Williams, K.P., Bixler, S.A., Ambrose, C.M., Garber, E.A., Miatkowski, K., et al. (1998). Identification of a palmitic acid-modified form of human Sonic hedgehog. J. Biol. Chem. *273*, 14037–14045.

Peters, P.J., Geuze, H.J., Van der Donk, H.A., Slot, J.W., Griffith, J.M., Stam, N.J., Clevers, H.C., and Borst, J. (1989). Molecules relevant for T cell-target cell interaction are present in cytolytic granules of human T lymphocytes. Eur. J. Immunol. *19*, 1469–1475.

Peters, P.J., Geuze, H.J., van der Donk, H.A., and Borst, J. (1990). A new model for lethal hit delivery by cytotoxic T lymphocytes. Immunol. Today *11*, 28–32.

Porter, J.A., Young, K.E., and Beachy, P.A. (1996). Cholesterol modification of Hedgehog signaling proteins in animal development. Science *274*, 255–259.

Raposo, G., Nijman, H.W., Stoorvogel, W., Liejendekker, R., Harding, C.V., Melief, C.J., and Geuze, H.J. (1996). B lymphocytes secrete antigen-presenting vesicles. J. Exp. Med. *183*, 1161–1172.

Reichsman, F., Smith, L., and Cumberledge, S. (1996). Glycosaminoglycans can modulate extracellular localization of the wingless protein and promote signal transduction. J. Cell Biol. *135*, 819–827.

Robbins, J.R., Barth, A.I., Marquis, H., de Hostos, E.L., Nelson, W.J., and Theriot, J.A. (1999). Listeria monocytogenes exploits normal host cell processes to spread from cell to cell. J. Cell Biol. *146*, 1333–1350.

Strigini, M., and Cohen, S.M. (2000). Wingless gradient formation in the *Drosophila* wing. Curr. Biol. *10*, 293–300.

Teleman, A.A., and Cohen, S.M. (2000). Dpp gradient formation in the *Drosophila* wing imaginal disc. Cell *103*, 971–980.

Tsuda, M., Kamimura, K., Nakato, H., Archer, M., Staatz, W., Fox, B., Humphrey, M., Olson, S., Futch, T., Kaluza, V., et al. (1999). The cell-surface proteoglycan Dally regulates Wingless signalling in Drosophila. Nature *400*, 276–280.

van den Heuvel, M., Nusse, R., Johnston, P., and Lawrence, P.A. (1989). Distribution of the wingless gene product in *Drosophila* embryos: a protein involved in cell-cell communication. Cell *59*, 739–749.

Zecca, M., Basler, K., and Struhl, G. (1996). Direct and long-range action of a wingless morphogen gradient. Cell *87*, 833–844.

Zitvogel, L., Regnault, A., Lozier, A., Wolfers, J., Flament, C., Tenza, D., Ricciardi-Castagnoli, P., Raposo, G., and Amigorena, S. (1998). Eradication of established murine tumors using a novel cell-free vaccine: dendritic cell-derived exosomes. Nat. Med. *4*, 594–600.